IJIE

INTERNATIONAL JOURNAL OF INTEGRATED ENGINEERING
ISSN: 2229-838X e-ISSN: 2600-7916

Vol. 18 No. 3 (2026) 48-62
https://publisher.uthm.edu.my/ojs/index.php/ijie

Catalytic Performance of NiO Loaded Eggshell-Derived CaO Prepared via Sol-Gel Technique in Pyrolysis of Mixed HDPE and PET

M.A.A. Mohamad Dzol[1], V. Balasundram[1]*, Norazana Ibrahim[2], Ruzinah Isha[3], Le Kim Pham Hoang[4]

[1] *Malaysia-Japan International Institute of Technology (MJIIT), Universiti Teknologi Malaysia, Jalan Sultan Yahya Petra, 54100 Kuala Lumpur, MALAYSIA*
[2] *Faculty of Chemical and Energy Engineering, Universiti Teknologi Malaysia, 81310 Johor Bahru, Johor, MALAYSIA*
[3] *Faculty of Chemical and Process Engineering Technology, Universiti Malaysia Pahang Al-Sultan Abdullah, 26300 Kuantan, Pahang, MALAYSIA*
[4] *Institute of Applied Technology and Sustainable Development, Nguyen Tat Thanh University, Ho Chi Minh City, 755414, VIETNAM*

*Corresponding Author: vekes@utm.my
DOI: https://doi.org/10.30880/ijie.2026.18.03.004

Article Info

Received: 31 January 2025
Accepted: 1 January 2025
Available online: 30 April 2026

Keywords

Plastic waste, pyrolysis, chicken eggshell, fuel, hydrocarbons

Abstract

This study investigates the catalytic pyrolysis of mixed high-density polyethylene (HDPE) and polyethylene terephthalate (PET) plastic waste utilizing nickel oxide (NiO) loaded on eggshell-derived calcium oxide (CaO-ce) as catalysts. The research aimed to evaluate the efficiency of various catalysts, including commercial CaO, CaO-ce, NiO, and a series of NiO loaded CaO-ce catalysts (NC1 to NC5), in producing liquid hydrocarbons from pyrolysis of HDPE and PET. The NC1 to NC5 catalysts were prepared via sol-gel technique and characterized for phase analysis, textural properties, surface morphology, and acidity. The study found that NC1 (5% of NiO and 95% of CaO-ce) achieved the highest pyrolysis oil yield of 58.01%, outpacing the non-catalytic HDPE-PET process and showcasing the extensive production of valuable hydrocarbons, especially in the C_{10}-C_{13} (28.74%) and C_{14}-C_{17} (26.23%) ranges. Additionally, NC1 and eggshell demonstrated superior catalytic efficiency, enhancing both the yield and quality of pyrolysis oil by increasing liquid hydrocarbon concentration and minimizing undesirable components like acids and furans. The findings underscore the potential of using nickel oxide loaded eggshell-derived calcium oxide as an effective catalyst in sustainable plastic waste management through catalytic pyrolysis, offering a pathway to recover valuable hydrocarbons while addressing environmental challenges associated with plastic waste accumulation.

1. Introduction

Plastic waste accumulation is a critical global issue with significant environmental, social, and economic consequences. The world produces over 400 million tons of plastic annually, with less than 10% being recycled

effectively [1]. The situation is alarming in Malaysia, with plastic waste constituting a significant portion of municipal solid waste. Improper disposal leads to environmental pollution, microplastic contamination, and adverse effects on ecosystems and human health [2]. High-density polyethylene (HDPE) and polyethylene terephthalate (PET) are among the most abundant plastic types in Malaysia and globally. HDPE is commonly used in products such as containers, pipes, and bottles due to its durability, while PET is widely used in packaging materials, especially for beverages [3]. Both plastics are non-biodegradable, making their accumulation a persistent problem that exacerbates the already critical waste management challenges.

Pyrolysis has emerged as a promising technology among the sustainable solutions for managing plastic waste [4]. Pyrolysis involves the thermal decomposition of plastics in an oxygen-free environment, converting them into valuable products such as liquid hydrocarbons, gaseous fuels, and char. This approach offers several advantages, such as it can process mixed or contaminated plastic waste, requires no pre-treatment, and recovers energy from fuels or chemicals [5]. The liquid hydrocarbons derived from pyrolysis mainly, have gained attention due to their potential use as feedstocks for fuel and petrochemical industries. However, the effectiveness of the pyrolysis process depends heavily on the choice of catalysts, which influence the cracking of polymer chains and the distribution of pyrolysis products [6]. The co-pyrolysis of these plastics presents additional complexity due to their distinct thermal degradation behaviours [7]. HDPE typically decomposes into long-chain hydrocarbons at high temperatures, while PET undergoes decarboxylation, releasing oxygenated compounds such as carbon dioxide and benzoic acid [8]. An effective catalyst must address these differences, ensuring efficient cracking and selective hydrocarbon production.

Catalytic pyrolysis, especially over acidic zeolite-based catalysts such as hydrogen-exchanged zeolite socony mobil five (HZSM-5), has been extensively studied due to its ability to enhance liquid hydrocarbon production [9]. HZSM-5 is highly efficient in breaking down long-chain polymers into valuable lighter hydrocarbons, particularly aromatics [10]. However, the highly efficient characteristics of zeolite catalysts makes them prone to deactivation through coke formation, reducing their activity and selectivity over prolonged use [11]. Moreover, their firm acidity can lead to undesired side reactions, including the formation of excessive gaseous and char products, which reduce liquid yields [12]. These limitations underscore the need for alternative catalysts that are efficient, environmentally friendly, and cost-effective.

Green catalysts derived from natural or waste materials, such as calcium oxide (CaO) from chicken eggshells, have emerged as viable alternatives in recent years [13]. Chicken eggshells, a readily available bio-waste, offer high calcium carbonate content, which can be thermally converted into CaO, a base catalyst [14]. CaO demonstrates excellent catalytic activity in pyrolysis due to its ability to promote cracking and decarboxylation reactions, leading to improved hydrocarbon yields [4]. Additionally, it is cost-effective, abundant, and aligns with the principles of waste valorization and circular economy. However, CaO alone may have limitations, including low surface area and pore volume, which can affect its catalytic performance [15].

To address these challenges, recent advancements involve the modification of CaO with metal oxides. Among the transition metal oxides, nickel oxides (NiO) are well-known for their ability to facilitate hydrogenation and cracking reactions, reducing the formation of coke and enhancing liquid product yields [16]. Incorporating these metal oxides onto the CaO support can create a synergistic effect, enhancing the overall catalytic activity, selectivity, and resistance to deactivation. Despite these promising developments, a critical research gap exists in the detailed understanding of how metal oxides modified CaO catalysts perform in the pyrolysis of mixed plastics, particularly HDPE and PET.

Currently, it was found the only few studies are available on the development of nickel oxides loaded calcium oxide from eggshell which was mainly used as catalysts and investigated in biodiesel production [17], hydrogen production [18], electrocatalytic oxidation [19], bio-template [20], and pyrolysis of food waste [21]. In addition, these catalysts were developed using incipient wetness impregnation, soaking and calcination, while, no studies focused on the development of nickel oxide loaded calcium oxide from eggshell via sol-gel method. The sol-gel method offers numerous advantages over the incipient wetness impregnation method when preparing catalysts. Firstly, the sol-gel technique allows for precise control over the chemical composition and uniform dispersion of metal oxide nanoparticles on the support matrix. This is due to the formation of a homogeneous sol, which ensures even distribution of the precursors during the gelation process, leading to enhanced catalytic activity and material performance.

Therefore, this study investigates the influence of nickel oxides loaded on calcium oxides from chicken eggshells as catalysts prepared via sol-gel method on the pyrolysis performance of mixed HDPE and PET. By evaluating product yields (oil, gas, char, and wax) and hydrocarbon selectivity, this research aims to identify the optimal conditions and catalyst formulation for maximizing liquid hydrocarbon production. This study addresses the pressing issue of plastic waste and advances the development of sustainable and cost-effective catalytic materials for energy recovery. In conclusion, this work bridges the knowledge gap between catalyst design and mixed-plastic pyrolysis, paving the way for scalable and green solutions to plastic waste management.

Int. Journal of Integrated Engineering Vol. 18 No. 3 (2026) p. 48-62

2. Methodology

2.1 Material

High-density polyethylene (HDPE) and polyethylene terephthalate (PET) plastic wastes were used as pyrolysis materials. HDPE and PET plastic wastes were collected from local waste management companies in Klang and Mantin, Malaysia. The obtained plastic resin samples were in pellet form at a 2 to 3 mm scale range. The samples were kept in a sealed container to avoid any contamination.

2.2 NiO Loaded CaO-ce

The synthesis of NiO/CaO was started by calcinating chicken eggshells into CaO (labelled as CaO-ce), which was used as a doper during sol-gel. The preparation of CaO-ce can be referred to in our previous work [22]. Secondly, citric [Sigma-Aldrich, 99.5 % purity] ($HOC(CO_2H)(CH_2CO_2H)_2$) was used to mix with deionized water and act as a chelating agent, where the Ni was detached from the percussor to form a soluble metal ion before adding the precursor for Ni in sol-gel using nickel (II) acetate tetrahydrate [Sigma-Aldrich, 98 % purity] ($Ni(CH_3CO_2)_2{\cdot}4\ H_2O$). Next, the nickel acetate tetrahydrate was added with CaO-ce to the mixture, and the pH changed from acid solution to alkali. Next, ethylene glycol [Merck, 99.5 % purity] ($(CH_2OH)_2$), which is an antifreeze formulation, was added as a stabilizing agent. When citric acid and ethylene glycol were mixed, it enhanced the reaction and promoted gel formation during the ageing period.

Finally, once the ageing period ends, the dry gel is crushed to obtain pre-calcined powder form and undergoes calcination to obtain the final product of NiO loaded CaO-ce. The commercial calcium oxide (CaO-com) (Purity = 100 %) was purchased from ACROS Organics for benchmarking. Table 1 shows the metal loading ratio. For comparison, nickel oxide (NiO) catalysts were produced to compare with NC1 to NC5 catalysts. Similar methodologies of physicochemical characterization of catalysts, such as phase analysis, elemental loadings, surface morphology, textural properties, and acidic properties, which were employed in our previous work [23].

Table 1 *Metal catalysts ratio between nickel oxide (NiO) and eggshell-derived calcium oxide (CaO-ce)*

Code	Nickel Oxide (NiO), wt%	Eggshell-derived Calcium Oxide (CaO-ce), wt%
NC1	5	95
NC2	10	90
NC3	15	85
NC4	20	80
NC5	25	75

2.3 Catalytic Pyrolysis of Mixed HDPE-PET

The pyrolizer was set up as shown in Fig. 1. The catalytic reactor is made up of a tube furnace; inside is a single crucible boat that was divided into two parts; one is for materials, and the other is for catalyst loading. The tube furnace at both ends is equipped with a release gauge or lever to control the intake and flow rate of nitrogen gas (N_2) at 50 mL/min and the condenser. The condenser is used to recover pyrolysis oil. The HDPE-PET mix plastic materials were fixed at a mass ratio 1:1, and pressure in the tube furnace was constantly maintained at 1 atm during operation. Firstly, the pyrolysis of mixed HDPE-PET was conducted at 500°C, followed by catalytic samples such as eggshell-derived calcium oxide (CaO-ce), commercial calcium oxide (CaO-com), nickel oxides (NiO), and nickel oxides loaded eggshell-derived calcium oxides (NC1 to NC5). Other setup details of this system can refer to our previous work [23].

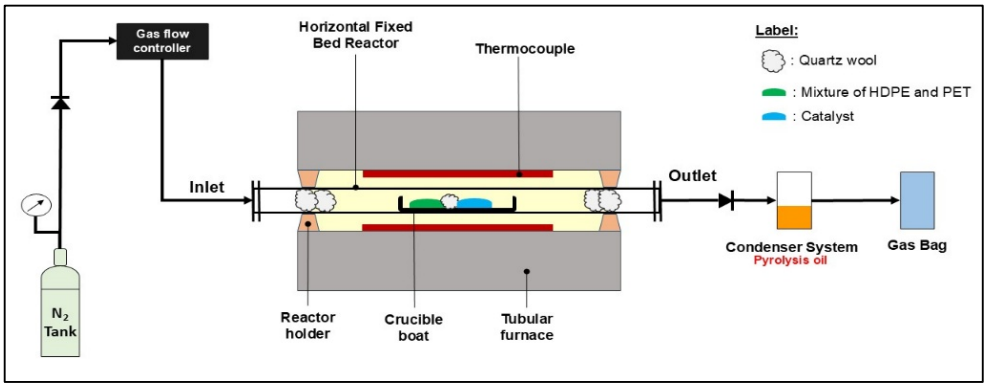

Fig. 1 *Fixed bed reactor pyrolizer*

3. Results and Discussions

3.1 Phase Analysis

The X-ray diffraction (XRD) patterns obtained for both commercial calcium oxide (CaO-com) and eggshells-derived calcium oxide (CaO-ce) reveal striking similarities, with prominent peaks observed at 2θ degree angles of 32.40°, 37.58°, 54.11°, 64.42°, and 67.62°, as depicted in Fig. 2 corresponding to the reference pattern of CaO (JCPDS No. 37-1497). This alignment suggests a substantial calcium oxide content in the chicken eggshells, consistent with the XRD signatures of commercial CaO. Thus, it can be reasonably inferred that the thermal treatment of calcium carbonate ($CaCO_3$) at 900°C in a muffle furnace leads to complete decomposition into CaO and CO_2. In a comparative context, similar findings by Liu et al. (2022) [24] regarding the thermal decomposition of $CaCO_3$ and the resultant formation of CaO corroborate the efficiency of this process in generating calcium oxide-based catalysts. Next, the XRD patterns for nickel oxide (NiO) exhibit distinct peaks at 2θ degrees of 37.62°, 43.50°, 63.06°, and 75.55°, indicative of NiO presence, as illustrated in Fig. 2 corresponding to the reference pattern of NiO (JCPDS No. 47-1049). These peaks of nickel oxide are aligned with our previous work [23]. Notably, the deposition of NiO onto the CaO-ce surface is discernible in samples NC1 to NC5, evidenced by the appearance of a characteristic NiO peak at 42.50° in the XRD spectra. A similar observation was reported by Zhang et al. (2022) [12] on distinct XRD peaks corresponding to deposited NiO on various substrates, highlighting the versatility of nickel-based catalysts in heterogeneous catalysis.

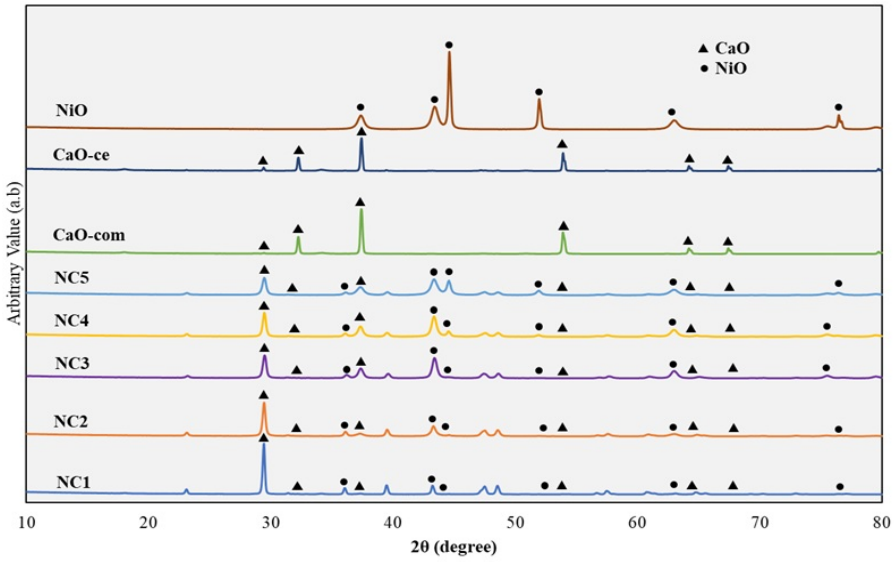

Fig. 2 *Phase analysis of CaO-com, CaO-ce, NiO, and NC1 to NC5*

In the NC1 to NC5 catalysts, overlapping peaks of CaO and NiO indicate the presence of separate crystalline phases, with no evidence of significant chemical interaction or new phase formation, such as mixed oxides or solid solutions. This suggests that the two components coexist as physically mixed phases. The effect of increasing NiO content is evident in the NC1 to NC5 samples. As the NiO loading increases from NC1 (5% NiO) to NC5 (25% NiO), the relative intensity of NiO peaks rises, confirming the proportional addition of NiO to the composite. At higher loadings, such as in NC5, the prominence of NiO peaks suggests reduced interaction with CaO, as the excess NiO primarily exists in its original crystalline phase. Notably, the preservation of CaO peaks across the NCx samples indicates that the CaO structure remains largely intact, even with the addition of NiO.

The XRD findings have significant implications for catalytic performance. The combination of NiO and CaO likely leads to a synergistic effect between the two components, as they remain distinct crystalline phases. The increasing NiO content enhances the availability of active NiO sites, potentially boosting catalytic activity. However, as in NC5, excessive NiO might overshadow the contribution of CaO, potentially altering key properties such as basicity. Overall, the analysis confirms that eggshell-derived CaO is a viable alternative to commercial CaO and highlights the tuneable catalytic properties of the nickel oxides modified eggshell, depending on the desired NiO-to-CaO ratio.

3.2 Surface Area and Pore Size Analysis

The data presented in Table 2 illustrates notable disparities in pore diameter, surface area, and pore volume among the different catalysts. Commercial calcium oxide (CaO-com) and eggshell-derived calcium oxide (CaO-ce) exhibited an identical pore diameter, averaging 3.72 nm. However, CaO-ce demonstrated superior surface area (8.72 m2/g) and total pore volume (0.0156 cm3/g) compared to CaO-com, which registered values of 3.80 m^2/g and 0.0063 cm^3/g, respectively similar observation can be found by Mmusi et al. (2021) [25]. In contrast, NiO exhibited substantially higher surface area and pore size characteristics, with a surface area of 18.13 m^2/g and a pore volume of 0.0860 cm^3/g, along with a pore diameter of 17.01 nm. These features enhance the accessibility of NiO active sites for catalytic activity, underscoring its efficacy as a catalyst for various applications. Furthermore, the incorporation of NiO into the CaO matrix led to a progressive increase in surface area and total pore volume across the NC1 to NC5 catalysts, spanning a range of 2.59 – 29.88 m2/g and 0.0219 – 0.1276 cm3/g, respectively similar observation can be found by Amal and Usman (2024) [17].

Table 2 *Textural properties of synthesized catalysts*

Catalysts	[a]S_{BET} (m^2/g)	[b]V_{total} (cm^3/g)	[c]D (nm)
CaO-com	3.80	0.0063	3.58
CaO-ce	8.72	0.0156	3.87
NiO	18.13	0.0860	17.01
NC1	2.59	0.0219	33.23
NC2	7.49	0.0305	10.63
NC3	11.23	0.0479	17.39
NC4	18.13	0.1276	20.41
NC5	29.88	0.1194	13.44

[a]S_{BET} (BET surface area) was obtained by the BET method.

[b]V_{total} (total pore volume) was obtained from the adsorbed amount at P/P0 = 0.99.

[c]D (pore diameter) was obtained from the adsorption branches of the isotherms by the BJH method.

Although NC5 exhibited a slight decrease in pore volume, its surface area remained significantly higher compared to NC1, reflecting the influence of NiO loading on pore structure evolution. Interestingly, the pore diameter of each catalyst displayed significant variations. For instance, the pore diameter of NC1 was measured at 33.23 nm, whereas NC2 exhibited a substantially smaller diameter of 10.63 nm. Pore diameters gradually increased from NC3 to NC4, reaching values of 17.39 nm and 20.41 nm, respectively, before experiencing a sudden drop to 13.44 nm for NC5. These variations in pore diameter underscore the intricate interplay between catalyst composition, synthesis parameters, and pore structure evolution. Overall, the data reveals that NiO addition significantly enhances the nickel oxides-modified eggshell's surface area and pore volume while reducing the pore diameter at higher loadings.

3.3 Surface Morphology

The surface morphology analysis depicted in Fig. 3 unveils distinctive characteristics of the synthesized catalysts. Fig.s 3 (A) and (B) illustrate the surface morphology of commercial calcium oxides (CaO-com) and eggshell-derived calcium oxides (CaO-ce), respectively, showcasing discernible differences in shape and porous structure.

CaO-com exhibits an irregular shape and agglomerated structure, indicative of its natural origin likely sourced from limestone quarries [26]. In contrast, CaO-ce presents a porous fibre rod-like structure attributed to the bio-mineralization process inherent in chicken eggshells, where proteins play a pivotal role in membrane formation [27]. Fig. 3 (C) provides insights into the surface morphology of NiO, revealing intricate mineralization and crystal growth patterns characteristic of the transformation from nickel acetate tetrahydrate to NiO [28]. In the modified sol-gel method, the ageing process facilitates gel penetration into the porous structure of CaO-ce, facilitating the deposition of NiO within the slits and interstices. This phenomenon is attributed to the calcination process, wherein chemical bonds are broken, leading to NiO/CaO catalysts forming, with oxidation serving as a stabilizing agent for Ni and Ca. Notably, an increase in NiO metal loading over CaO-ce results in a progressive deposition of NiO on the surface, as depicted in Fig. 3 (D) to (H). Fig. 3 (D) and (E) illustrate partial deposition of NiO on the porous surface of CaO-ce. In contrast, Fig.s 3 (F) to (H) depict increasingly higher levels of NiO deposition, eventually leading to the complete coverage of the surface. This phenomenon correlates with the metal loading content, wherein higher loading concentrations result in the filling and packing of porous textures with NiO, thereby diminishing the visibility of the porous structure at the nano-scale level.

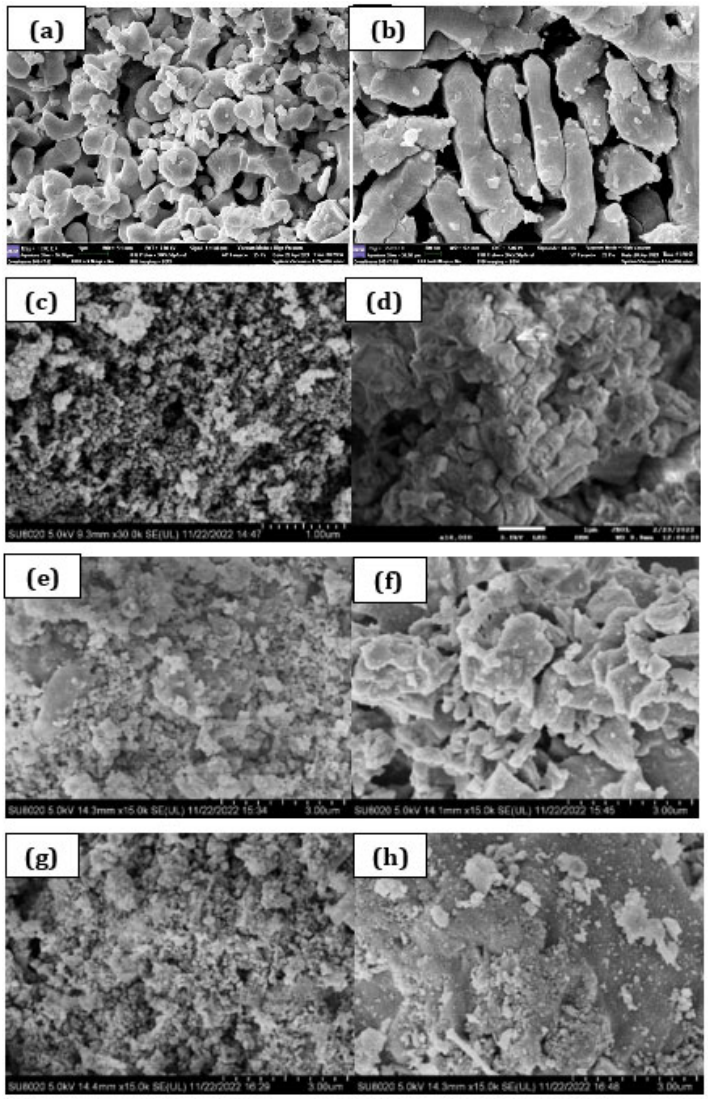

Fig. 3 *Surface morphology of (a) CaO-com; (b) CaO-ce; (c) NiO; (d) NC1; (e) NC2; (f) NC3; (g) NC4; and (h) NC5*

3.4 Acidic Analysis

Table 3 presents the acidic analysis of all catalysts, encompassing NiO, NC1, NC2, NC3, NC4, and NC5. The desorption peak areas [NH_3 (mmol/g)] indicate acid site concentrations, with the first peak representing weak acid sites and the second denoting strong acid sites. The total acid site content bears significant implications for

hydrocarbon yield outcomes, with a direct correlation observed between acid site abundance and the production of C_{10} to C_{13} hydrocarbons [4]. This underscores the pivotal role of acid site density in catalytic cracking processes, wherein higher acid site concentrations tend to enhance catalytic activity and hydrocarbon yield.

NiO exhibits a total acid site concentration of 0.8425 mmol/g, primarily dominated by Peak I (0.8147 mmol/g), indicating its substantial contribution from low-temperature acid sites. However, NiO shows negligible contributions from Peaks II and IV, and none from Peak III, suggesting limited diversity in acid site strength and type. For the NC1 to NC5 catalysts, the number of acid sites increases with higher NiO loadings. NC1, which contains the lowest NiO concentration, displays a total acid site concentration of 0.4528 mmol/g, with noticeable contributions from Peaks I (0.2798 mmol/g), II (0.0739 mmol/g), and III (0.0990 mmol/g). However, NC1 does not exhibit significant contributions from Peak IV. This indicates that low NiO content provides moderate acidity, sufficient for catalytic applications requiring a balance between low- and medium-strength acid sites.

Table 3 *The number of acid sites for each peak and the total number of acid sites for each catalyst*

Catalyst	Peak (I) acid sites NH_3 (mmol/g)	Peak (II) acid sites NH_3 (mmol/g)	Peak (III) acid sites NH_3 (mmol/g)	Peak (IV) acid sites NH_3 (mmol/g)	Total peak acid sites NH_3 (mmol/g)
NiO	0.8147	0.0278	-	-	0.8425
NC1	0.2798	0.0739	0.0990	-	0.4528
NC2	0.7244	0.2059	0.0095	0.2654	1.2052
NC3	0.3264	0.0879	0.0079	0.0296	0.4517
NC4	1.3239	0.1598	-	-	1.4837
NC5	1.6959	0.2684	-	-	1.9644

NC2 and NC3 show varying trends. NC2 has a total acid site concentration of 1.2052 mmol/g, attributed to significant contributions from Peak I (0.7244 mmol/g) and moderate contributions from Peaks II (0.2059 mmol/g) and IV (0.2654 mmol/g). This catalyst demonstrates higher diversity and strength in acid sites than NC1, suggesting improved catalytic potential for reactions requiring stronger acidity. Conversely, NC3 exhibits a total acid site concentration of 0.4517 mmol/g, with contributions from all peaks but at lower concentrations than NC2. This decrease in acidity suggests suboptimal loading of NiO in NC3. Lastly, NC4 and NC5, which have higher NiO concentrations, exhibit the highest total acid site concentrations, with NC4 at 1.4837 mmol/g and NC5 at 1.9644 mmol/g. Peak I dominates in both cases, contributing 1.3239 mmol/g for NC4 and 1.6959 mmol/g for NC5, indicating the substantial role of low-temperature acid sites. The absence of Peaks III and IV in NC4 and NC5 suggests that at higher NiO loadings, the diversity of acid sites diminishes, favouring low-strength acid sites. Similar findings were reported by Charisiou et al. (2019) [29].

Overall, the data suggests that increasing NiO content in NC1 to NC5 catalysts enhances the total number of acid sites, mainly through contributions from Peak I. However, the diversity of acid sites may decrease at higher NiO concentrations, as observed in NC4 and NC5. The optimal balance of acid site strength and diversity is seen in NC2, making it a promising catalyst for reactions requiring both low and medium-strength acid sites.

3.5 Catalytic Pyrolysis of HDPE and PET

3.5.1 Non-Catalytic, CaO-com, CaO-ce, and NiO

The pyrolysis of mixed HDPE and PET plastics, both non-catalytic and catalytic, provides valuable insights into optimizing the recovery of hydrocarbons from plastic waste. In non-catalytic pyrolysis, the distribution of products includes oil, gas, char, and wax, with the highest oil yield recorded at 36.45% as shown in Fig. 4. This indicates the effectiveness of thermal degradation in breaking down polymer chains into liquid hydrocarbons. However, the process is limited by a broad range of hydrocarbons produced without selectivity, resulting in significant char (23.01%) and wax (16.32%) yields due to incomplete decomposition. A similar observation was reported elsewhere, emphasizing the challenges associated with optimizing product selectivity in pyrolysis processes [28].

In contrast, as shown in Fig. 4, the catalytic pyrolysis shows a marked enhancement in product yields, particularly with commercial calcium oxides (CaO-com) and eggshell-derived calcium oxides (CaO-ce) catalysts, which increase oil yields to 67.00% and 64.19%, respectively. The improved performance is attributed to the base properties of CaO, which facilitate cracking and deoxygenation, especially for oxygenated compounds from PET. On the other hand, NiO produced a lower oil yield (34.63%) while yielding more gas (30.96%) and char (20.17%), highlighting its role in promoting secondary cracking and gasification reactions.

The wax yield is significantly reduced in catalytic pyrolysis when using CaO (6.88% and 9.93% for CaO-com and CaO-ce, respectively), demonstrating the catalyst's effectiveness in breaking down long-chain hydrocarbons into shorter ones. However, the wax yield remains relatively high with NiO (14.24%), suggesting inefficiencies in cracking or potential re-polymerization of intermediates. Gas production is notably higher with NiO, which supports hydrogenation and reforming reactions, though this is accompanied by increased char yield, indicating carbon deposition and incomplete polymer conversion. Overall, catalytic pyrolysis enhances oil yields and reduces wax formation compared to non-catalytic processes, addressing the latter's limitations.

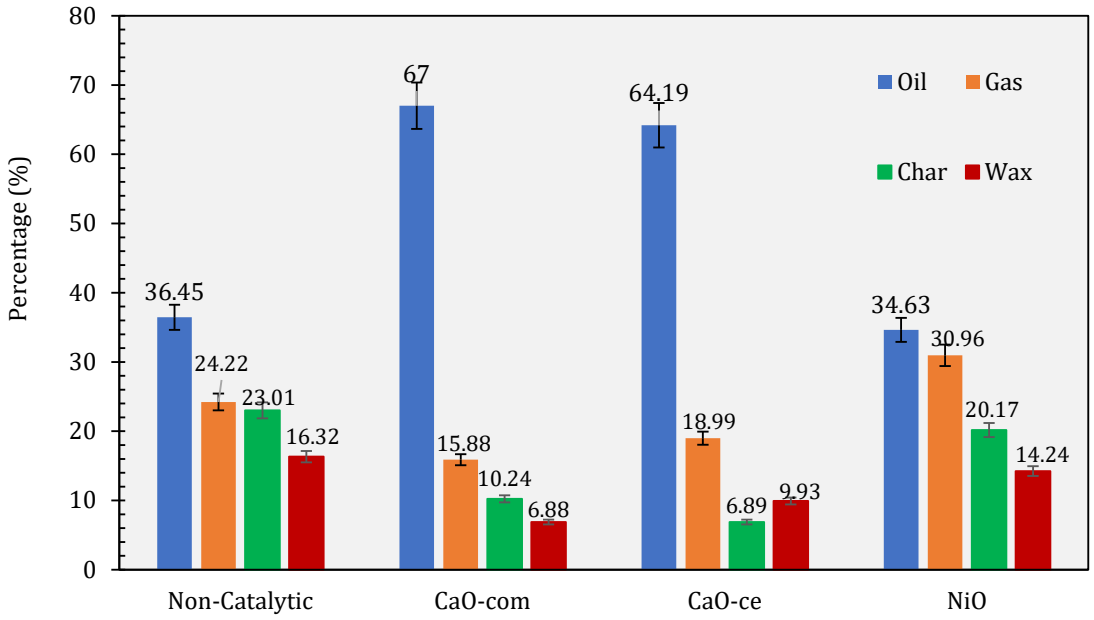

Fig. 4 *Pyrolysis product yield of non-catalytic and catalytic samples*

Table 4 shows the organic compositions produced in pyrolysis oil for non-catalytic and catalytic samples. It can be observed that the non-catalytic pyrolysis yields hydrocarbons at 42.30%, reflecting the decomposition of HDPE into long-chain alkanes and alkenes, which are valuable for fuel applications. Catalytic pyrolysis refines hydrocarbon selectivity, with NiO showing the highest hydrocarbon yield (40.14%). This superior performance can be attributed to NiO's high surface area (18.13 m^2/g) and pore volume (0.0860 cm^3/g) (refer Table 2), which enhance the availability of active sites for hydrocarbon formation. Conversely, CaO-ce, despite its superior surface area (8.72 m^2/g) compared to CaO-com (3.80 m^2/g), produces the lowest hydrocarbon yield (33.08%) due to its tendency to promote oxidation pathways. These findings underscore the interplay between catalyst structure and hydrocarbon production.

Table 4 *Organic composition of non-catalytic and catalytic samples*

Organic Compound	Non-Catalytic (%)	CaO-com (%)	CaO-ce (%)	NiO (%)
Hydrocarbons	42.30	39.91	33.08	40.14
Acids	49.35	46.85	52.82	45.89
Esters	2.29	-	5.79	6.26
Furans	4.60	5.41	-	4.62
Ketones	1.49	7.84	8.29	3.10

Next, it was found that the acids dominate the composition in both non-catalytic and catalytic processes. In non-catalytic pyrolysis, acids account for 49.35% of the product distribution, primarily due to the cleavage of ester linkages in PET, leading to carboxylic acids and other oxygenates. The catalytic systems show varying levels of acid formation, with CaO-ce producing the highest acid content (52.82%), surpassing that of CaO-com (46.85%) and NiO (45.89%). This result suggests that CaO-ce facilitates PET's depolymerisation and promotes secondary reactions that increase acidity. While acids are undesirable in pyrolysis oil due to their corrosive nature and

reduced stability, their formation in catalytic processes underscores the need for downstream upgrading techniques, such as esterification or neutralization, to improve oil quality.

The formation of esters is another notable aspect of catalytic pyrolysis, absent in the non-catalytic process (2.29%) with CaO-com but prominent in CaO-ce (5.79%) and NiO (6.26%). The presence of esters indicates that these catalysts actively catalyze esterification or transesterification reactions during pyrolysis, potentially involving intermediate carboxylic acids and alcohols. The higher ester content in NiO-based pyrolysis suggests its potential for producing value-added chemicals alongside hydrocarbons, albeit at the expense of reduced hydrocarbon selectivity. This observation further emphasizes the complex interplay of catalytic functionalities in tailoring the pyrolysis product distribution.

On the other hand, furans appear in moderate quantities (4.60%) in non-catalytic pyrolysis but vary significantly in catalytic systems. Furans are most prominent with CaO-com (5.41%), followed by NiO (4.62%), and are absent in CaO-ce. Their formation can be attributed to the stabilization of cyclic oxygenates during the intermediate stages of PET decomposition. While furans can serve as precursors for high-value chemicals, their oxygen content limits their utility as fuel components. The absence of furans in the CaO-ce system may indicate that this catalyst promotes alternative reaction pathways that do not favour cyclic oxygenates.

Ketones, often formed during the oxidative degradation of oxygen-rich plastics like PET, are present at low levels (1.49%) in non-catalytic pyrolysis but are significantly enhanced in catalytic processes. CaO-ce leads with the highest ketone production (8.29%), followed by CaO-com (7.84%) and NiO (3.10%). The elevated ketone content in CaO-ce systems underscores its catalytic propensity to promote oxidation pathways, likely through active sites that favour oxygenate stabilization. While ketones may detract from the fuel quality of pyrolysis oil, their presence highlights the potential for producing oxygenated chemical feedstocks.

Overall, the catalytic pyrolysis of HDPE-PET mixtures demonstrates a nuanced interplay between hydrocarbon and oxygenated compound formation dictated by the catalyst properties. NiO emerges as a promising catalyst for hydrocarbon-rich pyrolysis oils with moderate oxygenate content, while CaO-com provides a balanced product profile with hydrocarbons and acids. CaO-ce, with its distinct catalytic behaviour, offers opportunities for producing oxygenated compounds but requires process optimization to improve hydrocarbon yield. The insights gained from these catalytic systems are instrumental in advancing the design of pyrolysis technologies for tailored applications, including fuel production and chemical synthesis.

The hydrocarbon yield from the pyrolysis of mixed HDPE and PET illustrates the influence of both the pyrolysis mode (non-catalytic vs catalytic) and the catalyst type on the distribution of hydrocarbon fractions. The results reveal distinct patterns in the production of lighter hydrocarbons (C_6–C_9), medium-chain hydrocarbons (C_{10}–C_{13}), and longer hydrocarbons (C_{14}–C_{27}), reflecting the unique cracking efficiencies and mechanisms of the processes as shown in Fig. 5. In detail, it can be observed that the non-catalytic pyrolysis produces the lowest yield of C_6–C_9 hydrocarbons, at only 1.35%. This limited production indicates insufficient secondary cracking to generate short-chain hydrocarbons. Among the catalytic systems, CaO-com demonstrates the highest yield (5.71%), far exceeding those of CaO-ce (2.63%) and NiO (1.25%). The superior performance of CaO-com in this range can be attributed to its moderate surface area (3.80 m^2/g) and basicity, which likely enhance the cracking of longer chains into lighter hydrocarbons. The CaO-ce and NiO have a higher surface area, total pore volume, and diameter than CaO-com. Unfortunately, CaO-ce could not crack oxygenated and heavy hydrocarbon compounds into light C_6-C_9 hydrocarbons, as shown in Fig. 5. This might be due to the strong basic nature of CaO-ce. Similarly, NiO is well known for cracking; the low C_6-C_9 hydrocarbons might be due to the secondary cracking of these hydrocarbons into non-condensable gases, which ended with the highest gas yield at 30.96%, as shown in Fig. 4. Meanwhile, studies have shown that HZSM-5 promotes the formation of gasoline-range hydrocarbons (C_6–C_9) by facilitating secondary cracking and aromatization reactions. For instance, research on HDPE pyrolysis over HZSM-5 reports a hydrocarbon yield dominated by light fractions, with over 50% of the products in the gasoline range [23]. In contrast, CaO-based catalysts exhibit lower yields of C_6–C_9, indicating a lower degree of secondary cracking and a preference for middle distillates. This distinction highlights the benefit of CaO catalysts in producing diesel-range hydrocarbons while minimizing unwanted gas formation, a common issue with zeolites.

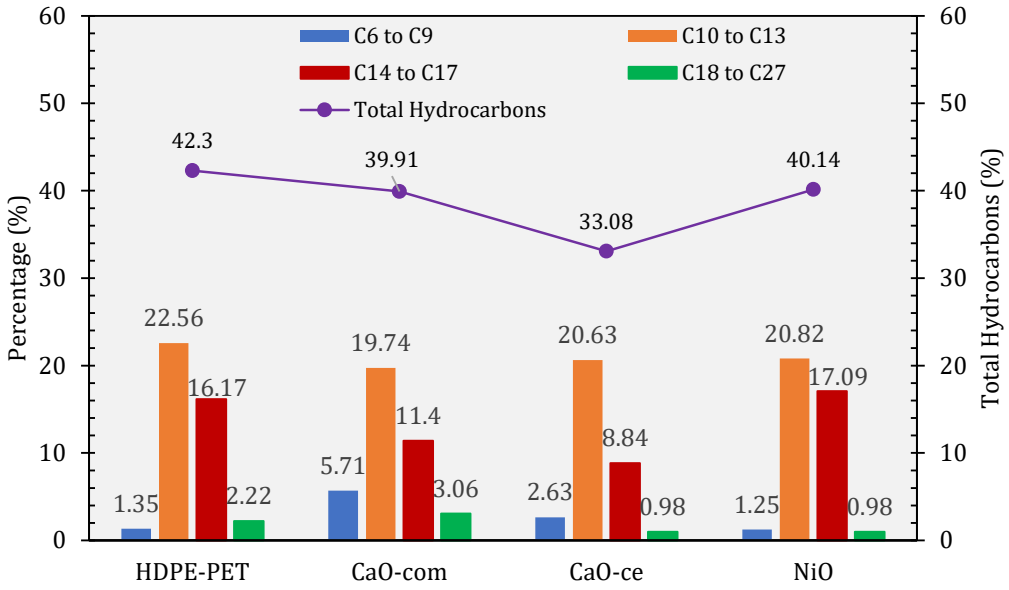

Fig. 5 *Hydrocarbon yield of non-catalytic and catalytic samples*

On the other hand, the C_{10}–C_{13} fraction dominates in both non-catalytic and catalytic pyrolysis processes, highlighting its suitability as a middle distillate fuel like kerosene or diesel. As shown in Fig. 5, the non-catalytic pyrolysis produces 22.56% of hydrocarbons in this range, primarily from the breakdown of HDPE into medium-chain alkanes and alkenes. Catalytically, NiO leads with 20.82%, followed closely by CaO-ce (20.63%) and CaO-com (19.74%). The comparable performance of NiO and CaO-ce underscores their effectiveness in medium-chain hydrocarbon production, likely due to their high surface area and accessible active sites. NiO, with a surface area of 18.13 m^2/g, provides numerous catalytic sites for controlled cracking, while CaO-ce's porous structure derived from eggshells facilitates intermediate chain degradation. The slightly lower yield from CaO-com may reflect its higher activity in producing lighter hydrocarbons (C_6–C_9) at the expense of the C_{10}–C_{13} fraction.

In the non-catalytic process, the C_{14}–C_{17} fraction constitutes 16.17%, arising from incomplete cracking of HDPE and PET. Catalytic systems, however, reveal varying efficiencies in this range. NiO again outperforms the others, with a yield of 17.09%, demonstrating its ability to stabilize longer-chain intermediates. CaO-com produces 11.40%, showing moderate activity in this fraction. In contrast, CaO-ce yields only 8.84%, likely due to its higher basicity and surface area, favouring oxygenate formation rather than hydrocarbon stabilization. The results suggest that NiO's unique crystalline structure and balanced acidity are crucial in optimizing the production of longer-chain hydrocarbons. The production of very long-chain hydrocarbons (C_{18}–C_{27}) is minimal in all systems, reflecting the tendency for cracking over extensive polymer chains. Non-catalytic pyrolysis generates only 2.22%, consistent with limited cracking efficiency. Among the catalytic systems, CaO-com produces the highest yield at 3.06%, followed by CaO-ce and NiO at 0.98%. CaO-com's superior performance in this fraction can be linked to its relatively low surface area and moderate pore volume, which reduce the secondary cracking of long chains. Conversely, the lower yields from CaO-ce and NiO suggest that their higher surface area promotes additional breakdown of long-chain hydrocarbons into medium and shorter fractions.

The total hydrocarbon yield reflects the effectiveness of the pyrolysis process in converting mixed plastics into fuel-grade products. Non-catalytic pyrolysis achieves 42.30%, highlighting the dominant contribution of HDPE. Among the catalytic systems, NiO achieves the highest overall yield at 40.14%, emphasizing its versatility in hydrocarbon production across all fractions. CaO-com follows closely at 39.91%, demonstrating balanced activity across light and long-chain hydrocarbons. CaO-ce, however, yields the lowest hydrocarbon content at 33.08% due to its higher basicity and surface area, favouring oxygenate and acid formation over hydrocarbon production.

In conclusion, while non-catalytic pyrolysis presents a promising method for plastic waste management, its inefficiencies necessitate further optimization. Catalytic pyrolysis offers a more efficient pathway for transforming mixed plastic waste into higher-quality hydrocarbons, with the choice of catalyst playing a critical role in optimizing product distributions and enhancing the sustainability of the pyrolysis process. The findings underscore the importance of selecting appropriate catalysts to balance the recovery of liquid oils and gaseous fuels based on desired end products.

Int. Journal of Integrated Engineering Vol. 18 No. 3 (2026) p. 48-62

3.5.2 NC1 to NC5 Catalysts

The distribution of pyrolysis products using catalysts with varying NiO-to-CaO-ce mass ratios (NC1 to NC5) is shown in Fig. 6. The results show that as the nickel content increases, the yield of pyrolysis oil decreases, with NC1 producing the highest oil yield at 58.01% and NC5 the lowest at 34.83%. This suggests that higher CaO-ce content favours oil production, possibly due to CaO's ability to enhance the cracking of larger molecules into liquid hydrocarbons. Conversely, the yield of pyrolysis gas increases with higher nickel content, with NC1 and NC5 producing at 23.00% and 32.10%, respectively. This indicates that nickel promotes gas formation, likely due to its catalytic properties favour plastic breakdown into smaller gaseous molecules. The yield of pyrolysis char also increases with higher nickel content, from 11.01% in NC1 to 17.08% in NC5, suggesting that nickel may enhance the formation of solid residues or inhibit the complete conversion of plastic. The yield of pyrolysis wax shows an interesting trend, increasing from NC1 (7.98%) to NC4 (16.04%) and slightly decreasing in NC5 (15.99%). The slight decrease in NC5 might indicate that excessive nickel content shifts the balance towards gas and char formation.

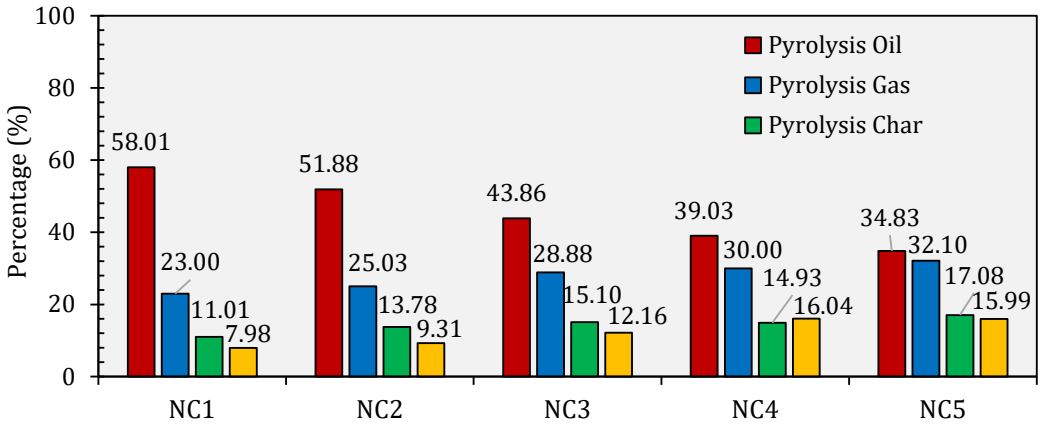

Fig. 6 *Pyrolysis product yield of NC1 to NC5 catalyst*

Table 5 shows the organic composition in pyrolysis oil using NC1 to NC5 catalysts. It can be observed that the relative content of hydrocarbons is highest in NC1 at 59.39%, indicating that lower nickel content is more effective in producing hydrocarbons. As the nickel content increases, the hydrocarbon content decreases, with NC5 having the lowest at 35.11%. This trend suggests that higher CaO content favours hydrocarbon production, possibly due to CaO's ability to enhance cracking reactions. This observation is consistent with the previous data, which shows that commercial calcium oxides (CaO-com) and eggshell-derived calcium oxides (CaO-ce) produced hydrocarbons more efficiently than NiO. The higher hydrocarbon yield in NC1 indicates that a lower NiO-to-CaO-ce ratio is more favourable for producing the desired pyrolysis oil.

Meanwhile, the relative content of acids increases with higher nickel content, peaking at 48.95% in NC5. This suggests that higher nickel content promotes the formation of acidic compounds during pyrolysis. NC2 and NC3 also show high acid content, indicating that intermediate NiO-to-CaO-ce ratios effectively produce acids. This trend aligns with the previous observation that higher nickel content favours the production of pyrolysis gas and char, as the formation of acids could result from incomplete plastic conversion into more stable hydrocarbons. Next, the content of esters is highest in NC5 at 8.11%, followed by NC2 at 7.40%. This indicates that higher nickel content favours ester formation, although the trend is not as clear-cut as with acids. NC1 has the lowest ester content at 2.50%, suggesting lower nickel content is less effective for ester production.

Table 5 *Organic composition of NC1 to NC5*

Organic Compound	Relative Content (%)				
	NC1	NC2	NC3	NC4	NC5
Acids	33.80	47.00	45.52	37.77	48.95
Esters	2.50	7.40	4.45	2.54	8.11
Furans	2.51	4.38	-	4.03	-
Hydrocarbons	59.39	41.21	42.85	53.22	35.11
Ketones	1.79	-	7.31	2.48	7.83

On the other hand, furans are present in NC1, NC2, and NC4, with the highest content in NC2 at 4.38%. The absence of furans in NC3 and NC5 suggests that certain NiO-to-CaO-ce ratios might inhibit their formation. This could be due to the specific catalytic properties of these ratios that favour other reactions over furan formation. The presence of furans in NC1 and NC2, which have lower nickel content, indicates that CaO might play a role in furan formation. Interestingly, ketones are present in NC1, NC3, NC4, and NC5, with the highest content in NC5 at 7.83%. The absence of ketones in NC2 suggests that certain NiO-to-CaO-ce ratios might not favour ketone formation. The higher content in NC3 and NC5 indicates that intermediate to high nickel content can promote ketone production. This could be due to the catalytic properties of nickel that favour the formation of oxygenated compounds like ketones. Hence, the nickel oxides loaded CaO-ce catalysts (NC1 to NC5) show a clear trend where increasing nickel content favours the formation of acids, esters, and ketones while decreasing the yield of hydrocarbons. This highlights the significant impact of catalyst composition on the organic composition of pyrolysis products.

Fig. 7 shows the percentage of hydrocarbon types in pyrolysis oil. It can be observed that, in the C_6 to C_9 fraction, NC4 has the highest content at 5.74%, followed by NC2 at 4.39%. Meanwhile, NC1 and NC5 have lower contents, suggesting that very low or very high nickel content is less favourable for this fraction. For the C_{10} to C_{13} fraction, NC1 has the highest content at 28.74%, followed by NC3 at 26.62%. This suggests that NC3 catalyst is effective in producing medium-chain hydrocarbons. The decrease in content with higher nickel ratios (NC5 at 21.78%) indicates that higher CaO content is more favourable for this fraction. Next, in the C_{14} to C_{17} fraction, NC1 has the highest content at 26.23%, indicating that lower nickel content is more effective in producing longer-chain hydrocarbons. The content decreases with higher nickel ratios, with NC5 having the lowest at 11.04%. This trend suggests that higher CaO content favours the production of longer-chain hydrocarbons. Lastly, for the C_{18} to C_{27} fraction, NC4 has the highest content at 3.93%, indicating that NC4 is more effective in producing very long-chain hydrocarbons. The lower contents in NC1 and NC5 suggest that very low or very high nickel content is less favourable for this fraction.

Yuan et al. (2022) found that plastic pyrolysis over HZSM-5 has shown a strong tendency to produce gasoline-range hydrocarbons (C_6–C_9), often exceeding 50% of the total hydrocarbon yield, as the zeolite's acidic sites promote extensive secondary cracking of longer-chain hydrocarbons. In contrast, the NC1 to NC5 catalysts exhibit lower C_6–C_9 production, with a maximum of 5.74% in NC4. This suggests that the CaO-based catalysts favour the preservation of middle and longer-chain hydrocarbons, making them more suitable for diesel-range fuel applications, whereas zeolites are more efficient in maximizing gasoline production through enhanced molecular breakdown.

Another key distinction is the influence of zeolites on aromatic hydrocarbon formation. The strong acidity and shape-selective properties of HZSM-5 favour the formation of aromatic compounds through cyclization and dehydrogenation reactions, leading to a higher fraction of monocyclic and polycyclic aromatic hydrocarbons (PAHs) [30]. Unfortunately, aromatics can enhance fuel properties, and excessive formation contributes to coke deposition, leading to catalyst deactivation. In contrast, the NiO-modified CaO-ce catalysts in this study demonstrate a lower tendency for aromatic formation, likely due to their weaker acidity and basic nature. This makes them more effective for producing straight-chain hydrocarbons with reduced secondary polymerization, which is particularly advantageous for liquid fuel applications requiring lower aromatic content.

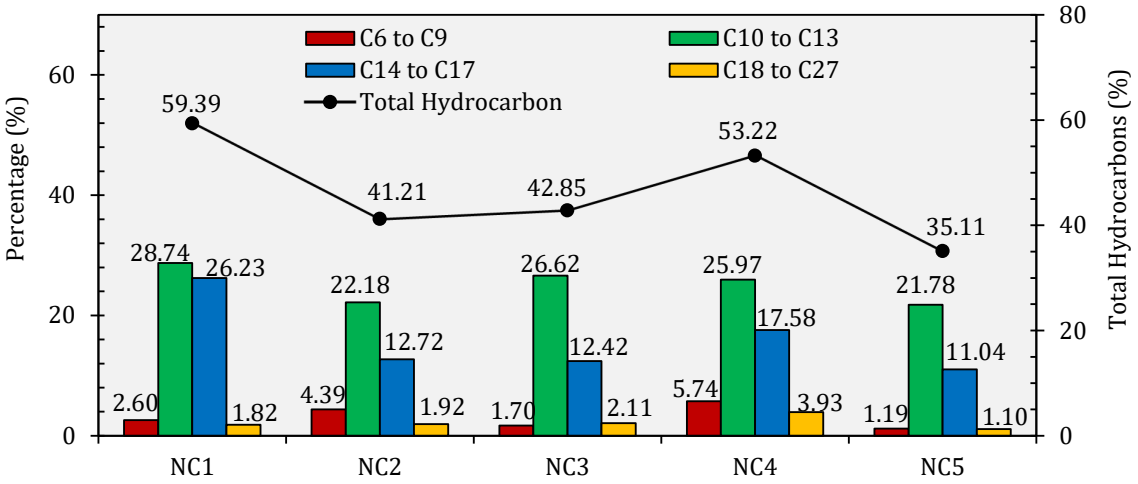

Fig. 7 *Hydrocarbon yield of NC1 to NC5*

4. Conclusion

This study critically evaluates the NiO loaded eggshell-derived CaO catalysts for the pyrolysis of mixed HDPE and PET plastics, addressing the pressing challenge of plastic waste valorization. The findings underscore the effectiveness of NC1, which achieved the highest pyrolysis oil yield (58.01%) and superior hydrocarbon selectivity, particularly in the C_{10}–C_{13} and C_{14}–C_{17} ranges. These fractions are crucial for high-value fuel applications, significantly advancing non-catalytic and conventional catalytic approaches. The study highlights the synergistic effects of NiO loading and CaO-ce's enhanced porosity, crystallinity, and acidity in promoting selective cracking and deoxygenation reactions. The porosity of CaO-ce plays a vital role in facilitating the diffusion of polymer chains and intermediate radicals, improving the accessibility of active sites, and enhancing catalytic activity. Higher surface area and pore volume in CaO-ce provide more active sites for thermal degradation, enabling more effective polymer fragmentation and reducing secondary polymerization, which can lead to char formation. Acidity and basicity are key factors influencing reaction pathways. The moderate acidity introduced by NiO loading enhances C-C and C-H bond cleavage, promoting selective cracking of long-chain hydrocarbons into valuable fuel fractions. At the same time, the inherent basicity of CaO-ce facilitates deoxygenation reactions. This balance between acidity and basicity ensures a more efficient catalytic conversion, favouring hydrocarbon selectivity over undesirable gas formation. NC1 demonstrated optimal performance, but higher NiO loading in NC5 revealed trade-offs, including increased gas production and diminished oil yields. Excessive NiO increases the number of acid sites, potentially leading to excessive cracking and promoting gasification rather than liquid fuel production. This illustrates the delicate balance required in catalyst design to optimize selectivity towards desired fuel fractions.

The use of bio-waste-derived catalysts aligns with circular economy principles, offering an environmentally friendly and cost-effective pathway for sustainable plastic waste management. The economic analysis indicates that nickel-loaded eggshell-derived CaO is a cost-effective and sustainable alternative to conventional zeolites for catalytic pyrolysis. The low-cost precursors (eggshells as waste material) and simple sol-gel synthesis significantly reduce production costs. However, zeolites offer better stability and reusability, making them more viable for long-term applications despite higher initial costs. For practical applications, the choice of catalyst should balance cost, catalytic activity, and reusability. If economic feasibility and waste valorization are the priorities, Ni/CaO is an excellent alternative. However, zeolites remain the preferred choice for industrial-scale applications requiring long-term stability. Future work should explore long-term catalyst stability, scalability, and the economic feasibility of implementing NiO-loaded CaO-ce catalysts in industrial settings. This study establishes a foundation for developing advanced catalytic materials, paving the way for transformative solutions to global plastic waste challenges.

Acknowledgement

A special thanks to the Ministry of Higher Education of Malaysia for the financial support to carry out this research project under the Fundamental Research University Grant (FRGS), Registration Proposal No: FRGS/1/2020/TK0/UTM/02/113 and Universiti Teknologi Malaysia (UTM) for the opportunity to carry out the research works.

Conflict of Interest

Authors declare that there is no conflict of interests regarding the publication of the paper.

Author Contribution

The authors confirm contribution to the paper as follows: ***study conception and design****: Vekes Balasundram;* ***data collection****: Muhammad Amir Aqil Mohamad Dzol, Norazana Ibrahim;* ***analysis and interpretation of results****: Muhammad Amir Aqil Mohamad Dzol, Ruzinah Isha, Le Kim Hoang Pham;* ***draft manuscript preparation****: Muhammad Amir Aqil Mohamad Dzol, Vekes Balasundram. All authors reviewed the results and approved the final version of the manuscript.*

References

[1] Liang, Y., Tan, Q., Song, Q., & Li, J. (2021, Jan 1). An analysis of the plastic waste trade and management in Asia. Waste Manag, 119, 242-253. https://doi.org/10.1016/j.wasman.2020.09.049

[2] Shaharudin, M. S., Fernando, Y., Ahmed, E. R., & Shahudin, F. (2020). Environmental Ngos Involvement in Dismantling Illegal Plastic Recycling Factory Operations in Malaysia. Journal of Governance and Integrity, 4(1), 29-36. https://doi.org/10.15282/jgi.4.1.2020.5610

[3] Zulkafli, A. H., Hassan, H., Ahmad, M. A., Din, A. T. M., & Wasli, S. M. (2023). Co-pyrolysis of biomass and waste plastics for production of chemicals and liquid fuel: A review on the role of plastics and catalyst types. Arabian Journal of Chemistry, 16(1), 104389. https://doi.org/10.1016/j.arabjc.2022.104389

[4] Chen, S., & Hu, Y. H. (2023). Chemical recycling of plastic wastes with alkaline earth metal oxides: A review. Science of The Total Environment, 167251. https://doi.org/10.1016/j.scitotenv.2023.167251

[5] Kartik, S., Balsora, H. K., Sharma, M., Saptoro, A., Jain, R. K., Joshi, J. B., & Sharma, A. (2022). Valorization of plastic wastes for production of fuels and value-added chemicals through pyrolysis–A review. Thermal Science and Engineering Progress, 32, 101316. Https://doi.org/10.1016/j.tsep.2022.101316

[6] Pan, D., Su, F., Liu, H., Liu, C., Umar, A., Castañeda, L., Algadi, H., Wang, C., & Guo, Z. (2021). Research progress on catalytic pyrolysis and reuse of waste plastics and petroleum sludge. ES Materials & Manufacturing. https://dx.doi.org/10.30919/esmm5f415

[7] Liew, J. X., Loy, A. C. M., Chin, B. L. F., AlNouss, A., Shahbaz, M., Al-Ansari, T., Govindan, R., & Chai, Y. H. (2021). Synergistic effects of catalytic co-pyrolysis of corn cob and HDPE waste mixtures using weight average global process model. Renewable Energy, 170, 948-963. https://doi.org/10.1016/j.renene.2021.02.053

[8] Bepari, M. R., Sullivan, L. R., O'Harra, K. E., Barbosa, G. D., Turner, C. H., & Bara, J. E. (2024). Depolymerizing Polyethylene Terephthalate (PET) via "Imidazolysis" for Obtaining a Diverse Array of Intermediates from Plastic Waste. ACS Applied Polymer Materials, 6(13), 7886-7896. https://doi.org/10.1039/d4lp00372a

[9] Soni, V. K., Singh, G., Vijayan, B. K., Chopra, A., Kapur, G. S., & Ramakumar, S. (2021). Thermochemical recycling of waste plastics by pyrolysis: a review. Energy & Fuels, 35(16), 12763-12808. https://doi.org/10.1021/acs.energyfuels.1c01292

[10] Sun, K., Zhang, L., Lin, Z., & Huang, Q. (2023). Alkaline earth metal-based minerals/wastes-catalyzed pyrolysis of poly (ethylene terephthalate)/poly (butylene terephthalate) for benzenes-enriched oil production. Waste Disposal & Sustainable Energy, 5(3), 269-282. https://doi.org/10.1007/s42768-023-00141-7

[11] Yuan, H., Li, C., Shan, R., Zhang, J., Wu, Y., & Chen, Y. (2022). Recent developments on the zeolites catalyzed polyolefin plastics pyrolysis. Fuel Processing Technology, 238, 107531. https://doi.org/10.1016/j.fuproc.2022.107531

[12] Zhang, F., Wang, F., Wei, X., Yang, Y., Xu, S., Deng, D., & Wang, Y.-Z. (2022). From trash to treasure: Chemical recycling and upcycling of commodity plastic waste to fuels, high-valued chemicals and advanced materials. Journal of Energy Chemistry, 69, 369-388. https://doi.org/10.1016/j.jechem.2021.12.052

[13] Yusuff, A. S., Gbadamosi, A. O., & Atray, N. (2022). Development of a zeolite supported CaO derived from chicken eggshell as active base catalyst for used cooking oil biodiesel production. Renewable Energy, 197, 1151-1162. https://doi.org/10.1016/j.renene.2022.08.032

[14] Laohavisuti, N., Boonchom, B., Boonmee, W., Chaiseeda, K., & Seesanong, S. (2021). Simple recycling of biowaste eggshells to various calcium phosphates for specific industries. Scientific Reports, 11(1), 15143. https://doi.org/10.1038/s41598-021-94643-1

[15] Hakim, K., Tan, E., Habib, S., Hafriz, R., & Salmiaton, A. (2024). Investigation of waste-derived and low-cost calcium oxide-based catalysts in co-pyrolysis of EFB-HDPE to produce high quality bio-oil. Journal of Analytical and Applied Pyrolysis, 177, 106375. https://doi.org/10.1016/j.jaap.2024.106375

[16] Ekeoma, B. C., Yusuf, M., Johari, K., & Abdullah, B. (2022). Mesoporous silica supported Ni-based catalysts for methane dry reforming: A review of recent studies. International Journal of Hydrogen Energy, 47(98), 41596-41620. https://doi.org/10.1016/j.ijhydene.2022.05.297

[17] Amal, R., & Usman, M. (2024). A review of breakthroughs in biodiesel production with transition and non-transition metal-doped CaO nano-catalysts. Biomass and Bioenergy, 184, 107158. https://doi.org/10.1016/j.biombioe.2024.107158

[18] Kim, Y., Cho, E., Ko, C.H. (2019). Preparation of Ni-based egg-shell-type catalyst on cylinder-shaped alumina pellets and its application for hydrogen production via steam methane reforming. Energy, 44(11), 5314-5323. https://doi.org/10.1016/j.ijhydene.2018.08.100

[19] Chi, X., Gao, L., Zhang, Y., Zhang, X., Hu, T. (2023). Nickel nanocrystals anchored nitrogen-doped carbon derived from eggshell membrane as an efficient catalyst for the electrocatalytic oxidation of urea. Applied Surface Science, 609, 155457. https://doi.org/10.1016/j.apsusc.2022.155457

[20] Venkatalakshmi, N., Kini, H.J., Naik, H.S.B. (2023). Eggshell Membrane Mediated Synthesis of CdO–NiO Nanocomposite for Multifunctional Applications. Journal of Inorganic and Organometallic Polymers and Materials, 33, 3221–3236. https://doi.org/10.1007/s10904-023-02757-y

[21] Valizadeh, S., Ko, C.H., Lee, J., Lee, S.H., Yu, Y.J., Show, P.L., Rhee, G.H., Park, Y. (2021). Effect of eggshell- and homo-type Ni/Al2O3 catalysts on the pyrolysis of food waste under CO2 atmosphere. Journal of Environmental Management, 294, 112959. https://doi.org/10.1016/j.jenvman.2021.112959

[22] Ali, N.S.M., Balasundram, V., Shameli, K., Ibrahim, N., Isha, R., & Manan, Z.A. (2021). The effect of calcium oxide from waste chicken eggshell on HZSM-5. Chemical Engineering Transactions, 89, 181-186. https://doi.org/10.3303/CET2189031

[23] Dzol, M.A.A.M., Balasundram, V., Shameli, K., Ibrahim, N., Manan, Z., Isha, R. (2022). Catalytic pyrolysis of high-density polyethylene over nickel-waste chicken eggshell/HZSM-5. Journal of Environmental Management, 324, 116392. https://doi.org/10.1016/j.jenvman.2022.116392

[24] Liu, J., Liu, M., Chen, S., Wang, B., Chen, J., Yang, D.-P., Zhang, S., & Du, W. (2022). Conversion of Au (III)-polluted waste eggshell into functional CaO/Au nanocatalyst for biodiesel production. Green Energy & Environment, 7(2), 352-359. https://doi.org/10.1016/j.gee.2020.07.019

[25] Mmusi, K. C., Odisitse, S., & Nareetsile, F. (2021). Comparison of CaO-NPs and chicken eggshell-derived CaO in the production of biodiesel from Schinziophyton rautanenii (Mongongo) nut oil. Journal of Chemistry, 2021, 1-15. https://doi.org/10.1155/2021/6663722

[26] Hargis, C. W., Chen, I. A., Devenney, M., Fernandez, M. J., Gilliam, R. J., & Thatcher, R. P. (2021). Calcium carbonate cement: A carbon capture, utilization, and storage (CCUS) technique. Materials, 14(11), 2709. https://doi.org/10.3390/ma14112709

[27] Rosaiah, P., Yue, D., Dayanidhi, K., Ramachandran, K., Vadivel, P., Eusuff, N. S., Reddy, V. R. M., & Kim, W. K. (2024). Eggshells & Eggshell Membranes–A Sustainable Resource for energy storage and energy conversion applications: A critical review. Advances in Colloid and Interface Science, 103144. https://doi.org/10.1016/j.cis.2024.103144

[28] El-Katori, E. E., Kasim, E. A., & Ali, D. A. (2022). Sol–gel synthesis of mesoporous NiO/ZnO heterostructure nanocomposite for photocatalytic and anticorrosive applications in aqueous media. Colloids and Surfaces A: Physicochemical and Engineering Aspects, 636, 128153. https://doi.org/10.1016/j.colsurfa.2021.128153

[29] Charisiou, N.D., Papageridis, K.N., Siakavelas, G., Sebastian, V., Hinder, S.J., Baker, M.A., Polychronopoulou, K., Goula, M.A. (2019). The influence of SiO2 doping on the Ni/ZrO2 supported catalyst for hydrogen production through the glycerol steam reforming reaction. Catalysis Today, 319, 206-219. https://doi.org/10.1016/j.cattod.2018.04.052

[30] Valizadeh, B., Valizadeh, S., Kim, H., Choi, Y.J., Seo, M.W., Yoo, K.S., Lin, K-Y.A., Hussain, M., Park, Y-K. (2024). Production of light olefins and monocyclic aromatic hydrocarbons from the pyrolysis of waste plastic straws over high-silica zeolite-based catalysts. Environmental Research, 245, https://doi.org/118076.10.1016/j.envres.2023.118076